Report

Cell Reports

Synaptotagmin-1 is a Ca^{2+} sensor for somatodendritic dopamine release

Graphical abstract

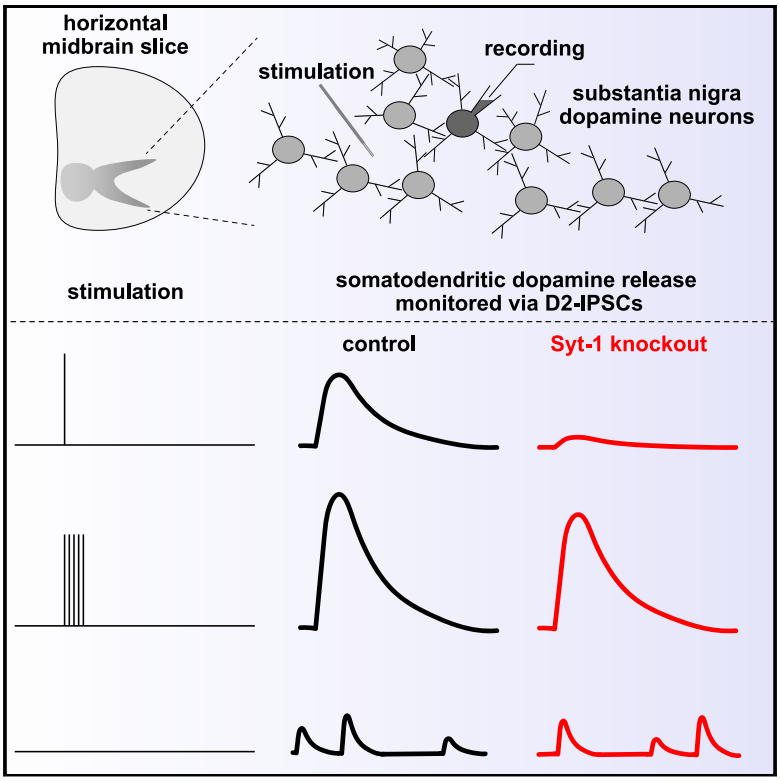

Highlights

- Somatodendritic dopamine release is assessed in Syt-1 knockout mice via D2-IPSCs
- Single action potential-evoked D2-IPSCs strongly depend on the fast Ca^{2+} sensor Syt-1
- High-frequency trains induce similar D2-IPSCs in Syt-1 knockout and control mice
- Spontaneous somatodendritic dopamine release is independent of Syt-1

Authors

Joseph J. Lebowitz, Aditi Banerjee, Claire Qiao, James R. Bunzow, John T. Williams, Pascal S. Kaeser

Correspondence

williamj@ohsu.edu (J.T.W.), kaeser@hms.harvard.edu (P.S.K.)

In brief

Lebowitz et al. show that synaptotagmin-1 is important for somatodendritic dopamine release triggered by single action potentials but not for spontaneous release or release evoked by high-frequency trains. Hence, multiple Ca^{2+} sensors mediate action-potential-evoked somatodendritic release in the midbrain with crucial roles for the fast, synchronous sensor synaptotagmin-1.

Lebowitz et al., 2023, Cell Reports *42*, 111915
January 31, 2023
https://doi.org/10.1016/j.celrep.2022.111915

CellPress

Cell Reports

CellPress
OPEN ACCESS

Report

Synaptotagmin-1 is a Ca^{2+} sensor for somatodendritic dopamine release

Joseph J. Lebowitz,[1] Aditi Banerjee,[2] Claire Qiao,[2] James R. Bunzow,[1] John T. Williams,[1,*] and Pascal S. Kaeser[2,3,*]
[1]Vollum Institute, Oregon Health and Science University, Portland, OR 97239, USA
[2]Department of Neurobiology, Harvard Medical School, Boston, MA 02115, USA
[3]Lead contact
*Correspondence: williamj@ohsu.edu (J.T.W.), kaeser@hms.harvard.edu (P.S.K.)
https://doi.org/10.1016/j.celrep.2022.111915

SUMMARY

Modes of somatodendritic transmission range from rapid synaptic signaling to protracted regulation over distance. Somatodendritic dopamine secretion in the midbrain leads to D2 receptor-induced modulation of dopamine neurons on the timescale of seconds. Temporally imprecise release mechanisms are often presumed to be at play, and previous work indeed suggested roles for slow Ca^{2+} sensors. We here use mouse genetics and whole-cell electrophysiology to establish that the fast Ca^{2+} sensor synaptotagmin-1 (Syt-1) is important for somatodendritic dopamine release. Syt-1 ablation from dopamine neurons strongly reduces stimulus-evoked D2 receptor-mediated inhibitory postsynaptic currents (D2-IPSCs) in the midbrain. D2-IPSCs evoked by paired stimuli exhibit less depression, and high-frequency trains restore dopamine release. Spontaneous somatodendritic dopamine secretion is independent of Syt-1, supporting that its exocytotic mechanisms differ from evoked release. We conclude that somatodendritic dopamine transmission relies on the fast Ca^{2+} sensor Syt-1, leading to synchronous release in response to the initial stimulus.

INTRODUCTION

Neuronal somata and dendrites are equipped with machinery to detect, transduce, and process neurotransmitter signals. However, many neurons also release neurotransmitters and neuromodulators through vesicular exocytosis from these compartments.[1,2] Somatodendritic exocytosis is involved in processes ranging from synaptic-like local signaling to paracrine regulation over long distances.[3–5] Distinct release profiles may be established by varying individual components of the exocytotic pathway, for example the transmitter-containing vesicles, the protein machinery that triggers exocytosis, or the structural organization of secretory sites at the somatodendritic membrane. The molecular organization and function of the various somatodendritic release pathways may be shared or specific depending on the neurotransmitter, necessitating detailed investigation of each transmitter.

An important form of somatodendritic exocytosis is that of dopamine in the midbrain, which underlies a transmission mode that controls the excitability of dopamine neurons.[6–10] We here focused on dissecting the Ca^{2+}-triggering mechanisms of somatodendritic dopamine release. At conventional synapses, release has been classified by its temporal relationship to action potential firing. Synchronous release is completed within milliseconds of presynaptic depolarization and is mediated by the fast Ca^{2+} sensors synaptotagmin-1 (Syt-1), Syt-2, and Syt-9.[11–15] Asynchronous release relies on the buildup of residual Ca^{2+}, persists for more than tens of milliseconds, and is triggered by additional Ca^{2+} sensors that include Syt-7.[16–20] Spontaneous release is independent of action potential firing, and its reliance on Ca^{2+} entry has remained uncertain, yet Ca^{2+} sensors including Syt-1 are important regulators of this form of release.[15,20–24]

In somatodendritic dopamine transmission, activation of D2 G protein-coupled receptors on dopamine neurons elicits an inhibitory postsynaptic current (D2-IPSC) that is carried by K^+ ions through the activation of G protein-gated inwardly rectifying K^+ (GIRK) channels.[7,9,10] A prevailing model has been that somatodendritic dopamine exocytosis uses distinct protein machinery compared with axonal dopamine release.[25,26] Specifically, while synchronous dopamine release from axons relies on Syt-1 and is rapid and precise,[27–29] somatodendritic release may have a different Ca^{2+} dependence, may rely on slower Ca^{2+} sensors, and may depend on Syt-7 and Syt-4.[30–33] This is consistent with some, but not all, aspects of somatodendritic dopamine signaling. For example, D2 receptor activation necessitates ~100 μM dopamine,[34] suggesting the need for synchronous exocytosis such that the extracellular dopamine concentration increases rapidly. In agreement, knockout of RIM, a protein that co-organizes release-ready vesicles with Ca^{2+} entry to accelerate release,[35–41] strongly impairs evoked somatodendritic dopamine transmission.[42] These data suggest rapid somatodendritic dopamine release mechanisms, but a suitable fast Ca^{2+} sensor has not been identified with confidence.

Here, we find that the fast Ca^{2+} sensor Syt-1 is important for evoked somatodendritic dopamine release. Conditional knockout of Syt-1 from dopamine neurons strongly reduced D2-IPSCs elicited by single stimuli, likely due to a decrease in vesicular release probability. This deficit was restored by viral re-expression of

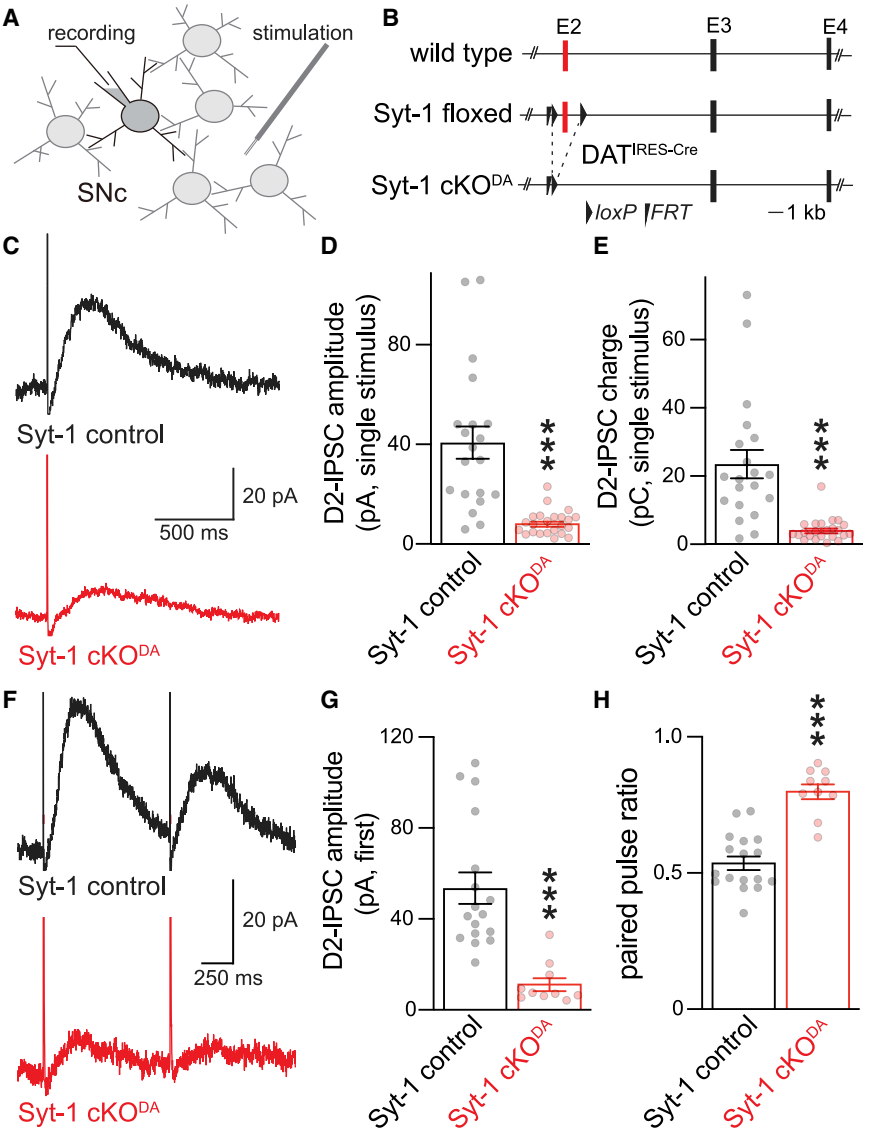

Figure 1. Somatodendritic dopamine release is strongly decreased in Syt-1 cKO^{DA} mice

(A and B) Schematic of recording (A) in the substantia nigra pars compacta (SNc) and of Syt-1 cKO^{DA} mice (B) generated as described before.[29] Exon numbers refer to coding exons.

(C–E) Example traces (C) and quantification of amplitude (D) and charge (E, area under the curve) of D2-IPSCs evoked by a single stimulus. Syt-1 control 20 cells/6 mice, and Syt-1 cKO^{DA} 23 cells/6 mice.

(F–H) Example traces of D2-IPSCs evoked by two electrical stimuli with a 1 s interval (F), and quantification of the first peak amplitude (G) and ratio of the amplitude of the second to the first D2-IPSC (H, paired pulse ratio). Syt-1 control 17 cells/7 mice, and Syt-1 cKO^{DA} 10 cells/4 mice.

Data are mean ± SEM; ***p < 0.005 as determined by Mann Whitney rank-sum tests (D, E, and G) or an unpaired Student's t test (H). For basal electrical properties, see Figure S1; for D2-IPSC rise times, see Figure S2.

Syt-1. High-frequency stimulus trains induced robust D2-IPSCs after Syt-1 ablation, indicating that an additional release pathway is activated. Lastly, Syt-1 knockout did not impair spontaneous D2-IPSCs and neither did lowering the extracellular Ca^{2+} concentration. We conclude that Syt-1 is a Ca^{2+} sensor for synchronous somatodendritic dopamine release. Additional sensors must be present in these mice to mediate transmission during repetitive activity after Syt-1 deletion, likely via asynchronous release. Spontaneous somatodendritic dopamine release is independent of Ca^{2+} and of the fast Ca^{2+} sensor Syt-1.

RESULTS

Syt-1 knockout strongly impairs somatodendritic dopamine release evoked by single stimuli

Of the known Ca^{2+} sensors, Syt-1 and Syt-7 are expressed in dopamine neurons.[43,44] We recently established that Syt-1 is a fast Ca^{2+} sensor for triggering axonal dopamine release.[29] Based on these data and on the properties of somatodendritic dopamine transmission, we hypothesized that Syt-1 triggers somatodendritic dopamine secretion. We performed electrophysiological recordings in brain slices (Figure 1A)[10,42] of mice with genetic ablation of Syt-1 selectively in dopamine neurons. We generated these mice though intercrossing of conditional, floxed Syt-1 mice[45] with DAT$^{IRES-Cre}$ mice[46] (Figure 1B) as described before.[29,47] In the following experiments, conditional knockout (cKO) mice for Syt-1 (Syt-1 cKO^{DA}) are mice with two floxed alleles for Syt-1 and a heterozygote DAT$^{IRES-Cre}$ allele, and Syt-1 control mice are littermate or age-matched mice from the same crossings with two wild type alleles for Syt-1 and a heterozygote DAT$^{IRES-Cre}$ allele. The basal electrical properties of dopamine neurons, including the tonic firing rate, series resistance, and capacitance, were not altered in brain slices of Syt-1 cKO^{DA} mice (Figure S1).

We determined if evoked somatodendritic dopamine release relies on Syt-1 (Figures 1 and S2). Release was monitored via D2-IPSCs, and we focused on the substantia nigra pars compacta (SNc) because axon collaterals are likely absent in the SNc, different from the ventral tegmental area (VTA).[48–50] Single electrical stimuli were applied through a stimulation electrode that was positioned ~50–100 μm away from a dopamine neuron recorded in whole-cell voltage clamp and held at −55 mV (Figure 1A). The average D2-IPSC amplitude and charge transfer evoked with a single stimulus were decreased by ~80% in Syt-1 cKO^{DA} mice, establishing that evoked somatodendritic dopamine release relies on Syt-1 (Figures 1C–1E). We next

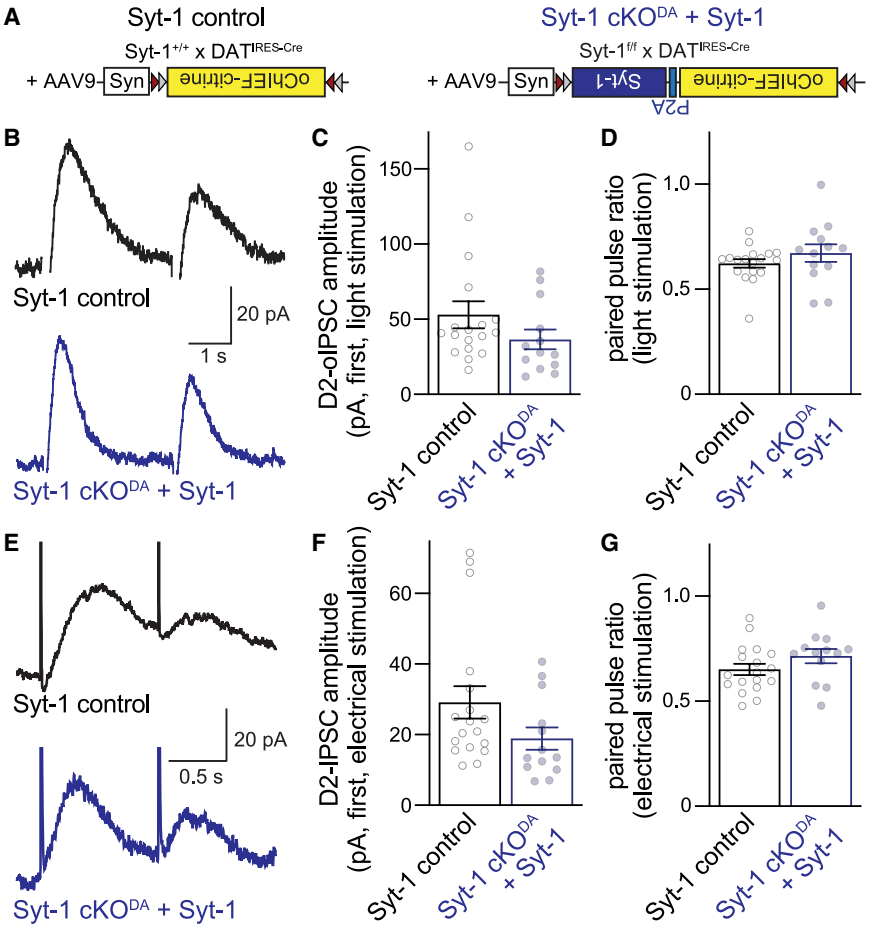

Figure 2. Syt-1 re-expression restores somatodendritic dopamine release in Syt-1 cKO^{DA} mice

(A) Strategy of rescue experiments.

(B–D) Example traces (B) and quantification of amplitude (C) and paired pulse ratio (D) of optogenetically induced D2-oIPSCs (two stimuli at 0.4 Hz) in control mice expressing oChIEF-citrine (Syt-1 control) and Syt-1 cKO^{DA} mice co-expressing oChIEF-citrine and Syt-1 (Syt-1 cKO^{DA} + Syt-1). Syt-1 control 18 cells/6 mice, and Syt-1 cKO^{DA} + Syt-1 13 cells/5 mice.

(E–G) As in (B)–(D) but for pairs of electrical stimuli (at 1 Hz) in the same cells; n as in (B)–(D).

Data are mean ± SEM; no significant differences were detected with Mann Whitney rank-sum tests (C, D, and F) or an unpaired Student's t test (G).

quantified the ratio of D2-IPSCs in response to two consecutive stimuli (paired pulse ratios) at 1 Hz (Figures 1F–1H). Previous work has shown that with paired stimuli, the second D2-IPSC is strongly depressed, similar to axonal dopamine release measured with different approaches.[27,51,52] In slices of Syt-1 control mice, the ratio was ~0.5 and was increased to ~0.8 in Syt-1 cKO^{DA} mice (Figures 1G and 1H). In synaptic physiology, paired pulse ratios are often used to estimate vesicular release probability, and they are inversely correlated with it.[53] Following this model, somatodendritic dopamine release has a high vesicular release probability that is mediated by the presence of Syt-1. Altogether, these experiments establish that evoked somatodendritic dopamine release is strongly decreased after Syt-1 ablation and suggest that Syt-1 is an important Ca^{2+} sensor for it.

Syt-1 re-expression restores somatodendritic dopamine release in Syt-1 cKO^{DA} mice

It is possible that Syt-1 is needed early in dopamine neuron development for maturation of the somatodendritic release machinery but that it does not directly act as a Ca^{2+} sensor for secretion. We sought to address this possibility by restoring somatodendritic release through re-expression of Syt-1 in adult Syt-1 cKO^{DA} mice. We constructed an adeno-associated virus (AAV) for Cre-dependent co-expression of Syt-1 and the fast channelrhodopsin variant oChIEF-citrine[54] using a 2A-based strategy (Figure 2A). The virus was produced as serotype 9 (AAV9) and was injected into the midbrain of Syt-1 cKO^{DA} mice to generate Syt-1 cKO^{DA} + Syt-1 mice. Syt-1 control mice were injected with a virus for Cre-dependent oChIEF-citrine expression (Figure 2A).

After 20 to 30 days of expression, we performed slice recordings in SNc areas with strong oChIEF-citrine fluorescence. To verify that the recorded neuron received inputs from dopamine neurons expressing the virus, two pulses of blue light were applied 2.5 s apart, and the optically induced D2 receptor-mediated IPSCs (D2-oIPSCs) were quantified (Figures 2B–2D). D2-oIPSCs were readily detected in both conditions, and the paired pulse ratio was indistinguishable. Hence, Syt-1 re-expression might restore somatodendritic dopamine release in Syt-1 cKO^{DA} mice. To test this, we measured electrically evoked D2-IPSCs (Figures 2E–2G) from the same cells used to record D2-oIPSCs (Figures 2B–2D). Robust D2-IPSCs were present in both conditions, and the paired pulse ratio was indistinguishable between Syt-1 control and Syt-1 cKO^{DA} + Syt-1 mice. In these analyses, we only included neurons with a D2-oIPSC equal to or greater than the D2-IPSC generated by a single electrical stimulus to select for cells with robust viral expression in the inputs. Altogether, the data indicate that Syt-1 re-expression restores most release in Syt-1 cKO^{DA} mice and support that Syt-1 operates as a Ca^{2+} sensor for somatodendritic dopamine secretion.

High-frequency trains induce robust somatodendritic release in Syt-1 cKO^{DA} mice

At conventional synapses, stimulus trains induce asynchronous glutamate or GABA release after Syt-1 knockout, and this asynchronous release is often sufficient to maintain synaptic charge transfer.[55,56] A release component that is Syt-1 independent was also detected for axonal dopamine release after Syt-1

ablation, but its detection with amperometry in striatal slices required blocking dopamine reuptake or strong depolarization via KCl.[29] *In vivo* microdialysis, a method that samples over long time periods and large striatal space, revealed robust *in vivo* dopamine levels in Syt-1 cKO^{DA} mice.[29] These observations might suggest that asynchronous release is sufficient to maintain dopamine secretion in response to repetitive stimulation after removing the fast Ca^{2+} sensor.

We probed whether repetitive stimulation induced somatodendritic dopamine release in the absence of Syt-1. First, we evoked D2-IPSCs with 5 pulses at 40 Hz in Syt-1 cKO^{DA} and control mice (Figures 3A–3D). These stimuli induced robust D2-IPSCs in Syt-1 cKO^{DA} slices, revealing that short trains restore a substantial amount of dopamine release. When we compared the relative increase of the 5-pulse D2-IPSC (Figure 3B) with the single-pulse D2-IPSC (Figure 1D, recorded from the same cells), we found a significantly greater increase in Syt-1 cKO^{DA} mice (Figure 3D). In Syt-1 control neurons, the 5-pulse D2-IPSC was ~3-fold greater than the single-pulse D2-IPSC, consistent with the depression observed in response to paired stimuli (Figure 1G). In Syt-1 cKO^{DA} neurons, the 5-pulse D2-IPSC was increased ~9-fold over the single-pulse D2-IPSC, establishing a strong enhancement. These data indicate that repetitive stimulation, likely via buildup of residual Ca^{2+}, triggers release through engaging additional Ca^{2+} sensors, at least in the Syt-1 cKO^{DA} mice.

The D2-IPSC can be depressed with 1-Hz stimulation, and it builds up rapidly when the stimulation frequency is switched to 100 Hz following this depression.[51] We investigated this by comparing Syt-1 cKO^{DA} with Syt-1 control mice (Figures 3E–3H). The overall charge during a 5-stimulus 1-Hz train was moderately decreased in Syt-1 cKO^{DA} slices compared with controls (Figure 3F). The D2-IPSCs evoked by 100-Hz 5-stimulus trains that followed the fifth stimulus at 1 Hz were comparable between Syt-1 cKO^{DA} and control slices (Figures 3G and 3H), similar to the 5-stimulus D2-IPSC at 40 Hz (Figures 3A–3D). These data support that a release pathway that is less dependent on Syt-1 is activated at high stimulus frequencies. Another fast, synchronous Ca^{2+} sensor is unlikely to mediate these D2-IPSCs because this sensor would be activated by single stimuli, which is largely excluded by the strong impairment of single-pulse D2-IPSCs (Figure 1). Instead, a slower, higher-affinity sensor is likely at play, possibly Syt-7 via mediating asynchronous release.[31]

Spontaneous somatodendritic dopamine release is Syt-1 independent

Midbrain dopamine neurons have spontaneous somatodendritic release that persists in the absence of action potential firing.[42,57] This is similar to conventional synapses, where miniature release events occur, are suppressed by the fast Ca^{2+} sensor Syt-1, and may be regulated by alternate Ca^{2+} sensors.[15,20–24] The exocytotic pathway for spontaneous somatodendritic dopamine release has not been well characterized, but it is vesicular and occurs at fusion sites that do not require the release site scaffold RIM.[42,57]

With the goal to improve detection of spontaneous D2-IPSCs, we overexpressed D2 receptors in the midbrain with AAVs (Figure 4A). We first tested whether evoked release is altered by D2 receptor overexpression (Figure S3). In both control and Syt-1 cKO^{DA} neurons, evoked D2-IPSCs and their paired pulse ratios were similar to the ones without overexpression (Figures 1, S3). D2 receptor overexpression greatly facilitated the detection of spontaneous events compared with previously published studies (Figure 4B).[42,57] We measured spontaneous D2-IPSCs at baseline, in low extracellular Ca^{2+}, and after blockade of action potential firing. In Syt-1 cKO^{DA} neurons, the frequencies and amplitudes of spontaneous D2-IPSCs were similar to controls (Figures 4B–4D). In both genotypes, reducing extracellular Ca^{2+} from 2.4 to 0.5 mM did not decrease event frequency or amplitude, nor did blockade of sodium channels with 1 μM TTX. We conclude that spontaneous somatodendritic dopamine release is independent of Syt-1. This is surprising because Syt-1 removal typically increases spontaneous event frequency at regular synapses.[15,22,24,58] These results underscore that evoked and spontaneous somatodendritic fusion events may not use the same release machinery[42] and bolster the model that distinct secretory pathways mediate evoked and spontaneous somatodendritic dopamine release.

DISCUSSION

We assessed Ca^{2+}-sensing mechanisms for the triggering of somatodendritic dopamine release and found that the fast Ca^{2+} sensor Syt-1 is important. Genetic ablation of Syt-1 in dopamine neurons strongly decreased D2-IPSCs evoked by a single stimulus, and viral re-expression of Syt-1 restored D2-IPSCs. D2-mediated transmission depresses during repetitive stimulation, supporting the model of a high initial release probability. After knockout of Syt-1, release during high-frequency stimulus trains was nearly normal, suggesting that Syt-1-independent release mechanisms respond to Ca^{2+} buildup. Spontaneous D2-IPSCs were unaffected by ablation of Syt-1, adding to a growing body of evidence indicating that spontaneous and evoked dopamine release are mediated by separate exocytotic pathways.

Comparison with previous work on somatodendritic and axonal release

Our work relates to earlier and recent studies on somatodendritic dopamine release. Based on the distinct Ca^{2+} dependence of somatodendritic and axonal dopamine release, and relying on knockdown experiments in cultured dopamine neurons, it was proposed that Syt-4 and Syt-7 are involved.[32,59] Indeed, constitutive double knockout of Syt-4 and Syt-7, but not knockout of Syt-7 alone, impaired somatodendritic dopamine release measured by voltammetry in brain slices.[30] It is noteworthy that vertebrate Syt-4 is unlikely a Ca^{2+} sensor as it lacks key Ca^{2+}-binding sites.[60,61] Two recent studies have confirmed roles for Syt-7 in somatodendritic release. One study found that the strong depression of D2-IPSCs during stimulus trains was alleviated by constitutive knockout of Syt-7.[62] The other[31] used Syt-7 antibodies or constitutive Syt-7 knockout to assess D2-IPSCs that may arise from autocrine signaling in which a dopamine neuron senses its own released dopamine.[63] Both manipulations impaired this form of transmission during short stimulus trains. Furthermore, Syt-1 antibodies applied through the recording

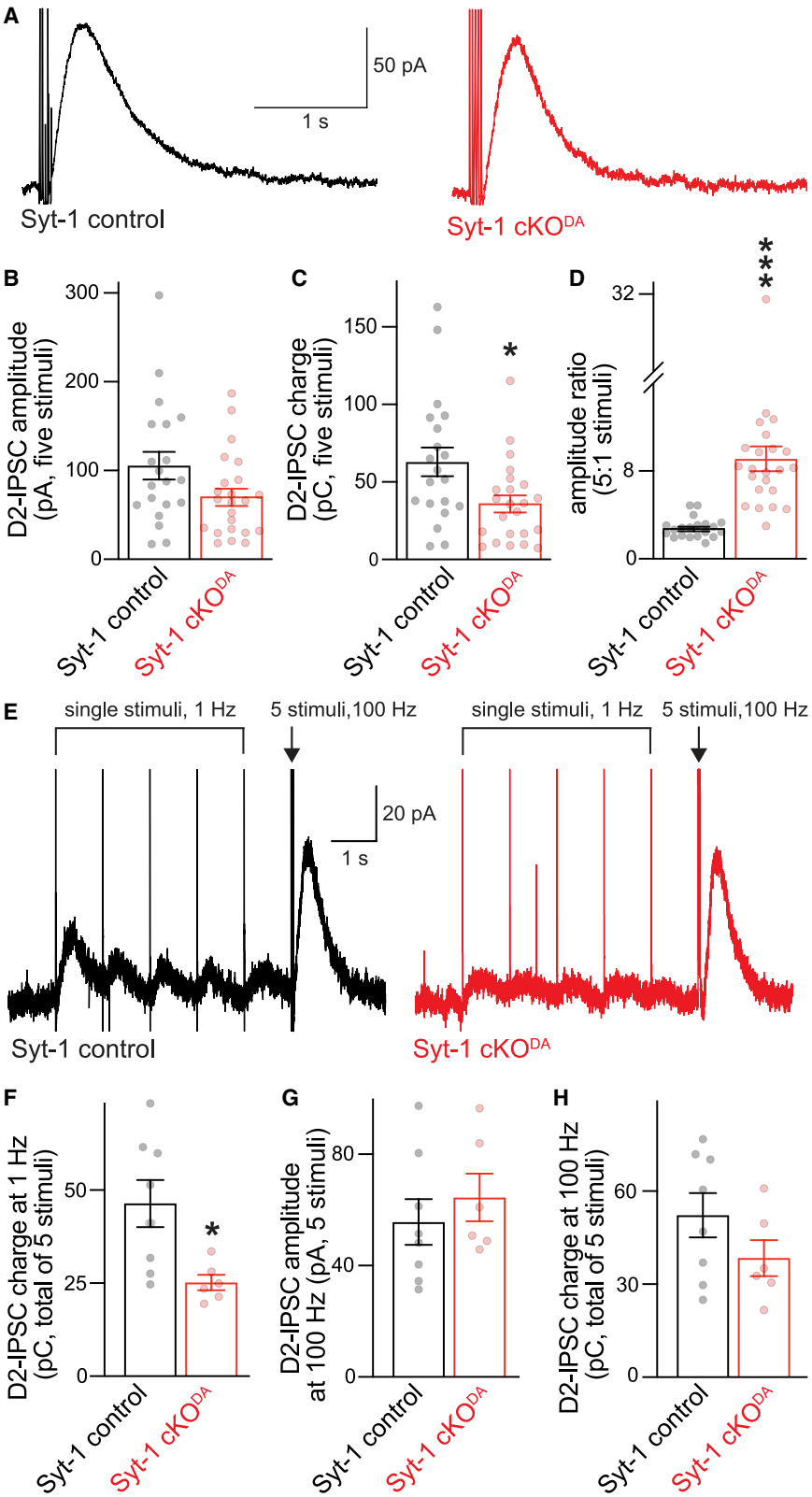

Figure 3. Somatodendritic dopamine release in response to stimulus trains

(A–D) Example traces (A) and quantification of amplitude (B) and charge (C, area under the curve) of D2-IPSCs evoked with a train of five electrical stimuli at 40 Hz, and ratio of the 5- to 1-stimulus D2-IPSC (D, single-stimulus amplitudes are from Figure 1C and were recorded in the same cells). Syt-1 control 20 cells/6 mice, and Syt-1 cKO^{DA} 23 cells/6 mice.

(E–H) Example traces of D2-IPSCs evoked by 5 stimuli at 1 Hz followed by a 5-stimulus train at 100 Hz (E), and quantification of the summed 5-stimulus D2-IPSC charge at 1 Hz (F), and the 5-stimulus amplitude (G) and charge (H) at 100 Hz. Syt-1 control 8 cells/3 mice, and Syt-1 cKO^{DA} 6 cells/2 mice.

Data are mean ± SEM; *p < 0.05, ***p < 0.005 as determined by Mann Whitney rank-sum tests (B–D) or unpaired Student's t tests (F–H).

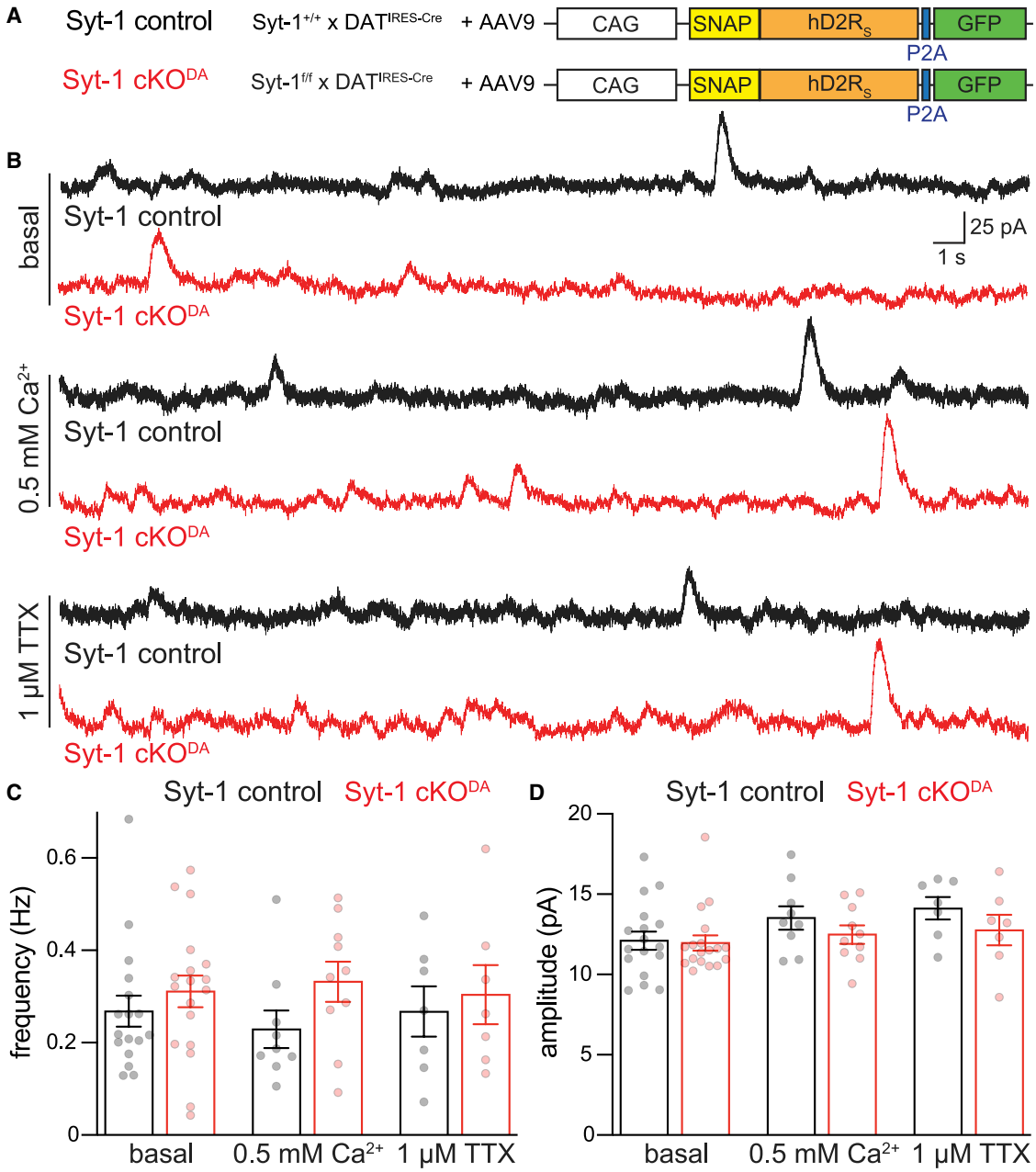

Figure 4. Spontaneous somatodendritic dopamine release is not detectably impaired by Syt-1 cKO^{DA}

(A) Strategy for AAV-mediated overexpression of D2 receptors (human, short version [hD2R$_S$]) in the midbrain.

(B–D) Example traces (B) and quantification of frequency (C) and amplitude (D) of spontaneous D2-IPSCs recorded in brain slices after viral expression of D2 receptors in basal recording conditions, after reducing extracellular Ca^{2+} from 2.4 to 0.5 mM, or following blockade of sodium channels with 1 µM TTX. Basal: Syt-1 control 17 cells/7 mice, and Syt-1 cKO^{DA} 18 cells/5 mice; 0.5 mM Ca^{2+}: Syt-1 control 9 cells/4 mice, and Syt-1 cKO^{DA} 10 cells/5 mice; 1 µM TTX: Syt-1 control 7 cells/6 mice, and Syt-1 cKO^{DA} 7 cells/4 mice.

Data are mean ± SEM; no significant differences were detected with two-way ANOVA. For evoked D2-IPSCs after D2 receptor overexpression, see Figure S3.

pipette impaired this autocrine transmission in response to a single stimulus, but it remained uncertain whether the antibody blocked Syt-1 function and whether Syt-1 controls the more commonly detected non-autocrine D2-IPSCs that we assessed here. Finally, Syt-1 knockout mice were also studied with voltammetry using either optogenetic or electrical stimulation, and mixed effects were observed with uncertain contributions of Syt-1 to somatodendritic release depending on the stimulation method.[64] Altogether, these recent studies support roles for Syt-7 in somatodendritic release. However, they did not allow for a decisive identification of the necessity and identity of the synchronous Ca^{2+} sensor for somatodendritic release.

The effect of Syt-1 deletion on evoked somatodendritic dopamine release (Figures 1, 2, and 3) resembles release deficits seen at classical synapses. At hippocampal synapses, Syt-1 ablation strongly impairs synchronous release, but the charge transfer during stimulus trains is maintained, and the resulting transmission is sufficient to support at least some aspects of behavior, for example memory acquisition.[55,56] The reliance on a fast Ca^{2+} sensor for midbrain dopamine transmission is counterintuitive since the speed of information transfer of this transmission mode is limited by G protein signaling, making it much slower than fast synaptic transmission.[9,65,66] A possible explanation is that synchronous dopamine release is needed to establish the high concentration of dopamine, ~100 μM, that is necessary for D2 receptor activation.[34,67]

Distinct release pathways for multiple modes of somatodendritic dopamine transmission

Our work defines the Ca^{2+}-triggering mechanism for synchronous somatodendritic dopamine release in response to the initial stimulus. The data also show that during stimulus trains, dopamine release recovers in the absence of Syt-1. Based on these findings, and building on previous work, we propose that somatodendritic dopamine release occurs through three exocytotic pathways. The first pathway is fast and synchronous and relies on the Ca^{2+} sensor Syt-1 (Figures 1 and 2) and the release site organizer RIM.[42] The second pathway is important during repetitive activity, for example burst firing, and it does not depend on Syt-1 (Figure 3). Secretion of this second pathway occurs at release sites organized by RIM, as RIM ablation abolishes it.[42] Some studies suggest that Syt-7 is involved.[30–32,62] This transmission mode is likely mediated by asynchronous release in response to build up of Ca^{2+} during repetitive activity, consistent with roles of Syt-7, a Ca^{2+} sensor for asynchronous release at synapses.[16,17,20] Finally, previous work[42,57] and our data (Figure 4) uncover the presence of a spontaneous dopamine release pathway that is independent of action potential firing and is not sensitive to lowering extracellular Ca^{2+} or to removing Syt-1 or RIM.

Together, these studies reveal the distinct involvement of specific proteins, Syt-1, Syt-7, and RIM, in synchronous, asynchronous, and spontaneous somatodendritic dopamine release. It is interesting to assess how these distinct molecular requirements could reflect distinct cell biological pathways for secretion. While Syt-1 is a key component of synaptic vesicles,[68,69] Syt-7 is not localized on synaptic vesicles but instead at the target membrane or on different intracellular membrane compartments.[70,71] The identity of the intracellular compartment for somatodendritic dopamine secretion remains uncertain. Early studies established that somatodendritic dopamine release depends on SNARE proteins[25,72] and on Ca^{2+},[10,32,33,59,73,74] indicating that exocytosis underlies this form of release. Classical work further suggested that tubulo-vesicular structures, rather than small synaptic vesicles, may be involved.[75–77] Together, these studies and our work raise the possibility that multiple membrane compartments mediate somatodendritic dopamine release: small synaptic vesicles with Syt-1 may account for the initial synchronous component, while release in response to high-frequency trains, and possibly spontaneous release, may be supported by tubulo-vesicles or other compartments. This model may also explain why the asynchronous component is difficult to detect in experiments assessing axonal release.[29] It is possible that axonal release is dominated by small clear vesicles, which densely occupy the dopamine axon.[78–80]

Limitations of the study

Our work reveals important roles for Syt-1 in somatodendritic dopamine release. One limitation to the interpretation of our work is that morphological characterization of the underlying signaling structure remains difficult. Release site architecture and release-receptor assemblies have not been visualized, the intracellular membrane compartments that undergo exocytosis remain uncertain, and it was not possible to determine whether exogenously expressed proteins, for example D2 receptors or Syt-1, localize like the endogenous counterparts. In the VTA, but less likely in the SNc, axon collaterals might be present as well. Hence, models on the molecular and cellular organization of this release mode can currently only be inferred from functional experiments like the one presented here, characterizing transmission deficits after gene knockout. Localizing Syt-1 and other proteins for somatodendritic transmission remains a future goal. In addition, the D2-IPSC measurements used here differ from axonal release measurements with electrochemical detection and from measurements of synaptic transmission monitored via ionotropic receptors. It is difficult to directly compare effect magnitudes across methods, and it remains uncertain whether classical concepts of synaptic transmission, for example on the inverse relationship of paired pulse ratios and vesicular release probability, fully apply. Nevertheless, our experiments establish that Syt-1 is critical for somatodendritic dopamine release evoked by single action potentials.

STAR★METHODS

Detailed methods are provided in the online version of this paper and include the following:

- KEY RESOURCES TABLE
- RESOURCE AVAILABILITY
  - Lead contact
  - Materials availability
  - Data and code availability
- EXPERIMENTAL MODEL AND SUBJECT DETAILS
  - Animals
  - Cell lines
- METHOD DETAILS
  - Molecular biology and production of AAV viruses
  - Stereotaxic viral delivery
  - Brain slice preparation
  - Electrophysiological recordings in brain slices
- QUANTIFICATION AND STATISTICAL ANALYSIS

SUPPLEMENTAL INFORMATION

Supplemental information can be found online at https://doi.org/10.1016/j.celrep.2022.111915.

ACKNOWLEDGMENTS

We thank all members of the Kaeser and Williams laboratories for insightful discussions and feedback. This work was supported in part by the NIH (R01NS103484 and R01NS083898, P.S.K., and R01DA004523 and T32DA 007262, J.T.W.), an Alice and Joseph Brooks fellowship (A.B.), and Harvard Medical School (P.S.K.).

AUTHOR CONTRIBUTIONS

Conceptualization, J.J.L., A.B., J.T.W., and P.S.K.; methodology, J.J.L., A.B., C.Q., J.R.B., and J.T.W.; formal analysis, J.J.L., J.T.W., and P.S.K.; investigation, J.J.L. and J.T.W.; resources, A.B., C.Q., and J.R.B.; writing – original draft, J.J.L., J.T.W., and P.S.K.; writing – review & editing, J.J.L., A.B., C.Q., J.R.B., J.T.W., and P.S.K.; supervision, J.T.W. and P.S.K.; funding acquisition, J.T.W. and P.S.K.

DECLARATION OF INTERESTS

Claire Qiao is currently a graduate student at Peking University.

Received: July 10, 2022
Revised: November 7, 2022
Accepted: December 13, 2022

REFERENCES

1. Kennedy, M.J., and Ehlers, M.D. (2011). Mechanisms and function of dendritic exocytosis. Neuron *69*, 856–875. https://doi.org/10.1016/j.neuron.2011.02.032.
2. Pang, Z.P., and Südhof, T.C. (2010). Cell biology of Ca2+-triggered exocytosis. Curr. Opin. Cell Biol. *22*, 496–505. https://doi.org/10.1016/j.ceb.2010.05.001.
3. Isaacson, J.S., and Strowbridge, B.W. (1998). Olfactory reciprocal synapses: dendritic signaling in the CNS. Neuron *20*, 749–761. https://doi.org/10.1016/s0896-6273(00)81013-2.
4. Cheramy, A., Leviel, V., and Glowinski, J. (1981). Dendritic release of dopamine in the substantia nigra. Nature *289*, 537–542.
5. Son, S.J., Filosa, J.A., Potapenko, E.S., Biancardi, V.C., Zheng, H., Patel, K.P., Tobin, V.A., Ludwig, M., and Stern, J.E. (2013). Dendritic peptide release mediates interpopulation crosstalk between neurosecretory and preautonomic networks. Neuron *78*, 1036–1049. https://doi.org/10.1016/j.neuron.2013.04.025.
6. Ludwig, M., Apps, D., Menzies, J., Patel, J.C., and Rice, M.E. (2016). Dendritic release of neurotransmitters. In Comprehensive Physiology (John Wiley & Sons, Inc.), pp. 235–252. https://doi.org/10.1002/cphy.c160007.
7. Ford, C.P. (2014). The role of D2-autoreceptors in regulating dopamine neuron activity and transmission. Neuroscience *282*, 13–22. https://doi.org/10.1016/j.neuroscience.2014.01.025.
8. Crocker, A.D. (1997). The regulation of motor control: an evaluation of the role of dopamine receptors in the substantia nigra. Rev. Neurosci. *8*, 55–76. https://doi.org/10.1515/REVNEURO.1997.8.1.55.
9. Gantz, S.C., Ford, C.P., Morikawa, H., and Williams, J.T. (2018). The evolving understanding of dopamine neurons in the substantia nigra and ventral tegmental area. Annu. Rev. Physiol. *80*, 219–241. https://doi.org/10.1146/annurev-physiol-021317-121615.
10. Beckstead, M.J., Grandy, D.K., Wickman, K., and Williams, J.T. (2004). Vesicular dopamine release elicits an inhibitory postsynaptic current in midbrain dopamine neurons. Neuron *42*, 939–946. https://doi.org/10.1016/j.neuron.2004.05.019.
11. Xu, J., Mashimo, T., and Südhof, T.C. (2007). Synaptotagmin-1, -2, and -9: Ca2+ sensors for fast release that specify distinct presynaptic properties in subsets of neurons. Neuron *54*, 567–581. https://doi.org/10.1016/j.neuron.2007.05.004.
12. Fernández-Chacón, R., Königstorfer, A., Gerber, S.H., García, J., Matos, M.F., Stevens, C.F., Brose, N., Rizo, J., Rosenmund, C., Südhof, T.C., et al. (2001). Synaptotagmin I functions as a calcium regulator of release probability. Nature *410*, 41–49. https://doi.org/10.1038/35065004.
13. Geppert, M., Goda, Y., Hammer, R.E., Li, C., Rosahl, T.W., Stevens, C.F., and Südhof, T.C. (1994). Synaptotagmin I: a major Ca2+ sensor for transmitter release at a central synapse. Cell *79*, 717–727.
14. Chapman, E.R., Hanson, P.I., An, S., and Jahn, R. (1995). Ca2+ regulates the interaction between synaptotagmin and syntaxin 1. J. Biol. Chem. *270*, 23667–23671.
15. Broadie, K., Bellen, H.J., DiAntonio, A., Littleton, J.T., and Schwarz, T.L. (1994). Absence of synaptotagmin disrupts excitation-secretion coupling during synaptic transmission. Proc. Natl. Acad. Sci. USA *91*, 10727–10731. https://doi.org/10.1073/pnas.91.22.10727.
16. Wen, H., Linhoff, M.W., McGinley, M.J., Li, G.-L., Corson, G.M., Mandel, G., and Brehm, P. (2010). Distinct roles for two synaptotagmin isoforms in synchronous and asynchronous transmitter release at zebrafish neuromuscular junction. Proc. Natl. Acad. Sci. USA *107*, 13906–13911. https://doi.org/10.1073/pnas.1008598107.
17. Bacaj, T., Wu, D., Yang, X., Morishita, W., Zhou, P., Xu, W., Malenka, R.C., and Südhof, T.C. (2013). Synaptotagmin-1 and synaptotagmin-7 trigger synchronous and asynchronous phases of neurotransmitter release. Neuron *80*, 947–959. https://doi.org/10.1016/j.neuron.2013.10.026.
18. Sun, J., Pang, Z.P., Qin, D., Fahim, A.T., Adachi, R., Südhof, T.C., and Sudhof, T.C. (2007). A dual-Ca2+-sensor model for neurotransmitter release in a central synapse. Nature *450*, 676–682. https://doi.org/10.1038/nature06308.
19. Yao, J., Gaffaney, J.D., Kwon, S.E., and Chapman, E.R. (2011). Doc2 is a Ca2+ sensor required for asynchronous neurotransmitter release. Cell *147*, 666–677. https://doi.org/10.1016/j.cell.2011.09.046.
20. Kaeser, P.S., and Regehr, W.G. (2014). Molecular mechanisms for synchronous, asynchronous, and spontaneous neurotransmitter release. Annu. Rev. Physiol. *76*, 333–363. https://doi.org/10.1146/annurev-physiol-021113-170338.
21. Groffen, A.J., Martens, S., Díez Arazola, R., Cornelisse, L.N., Lozovaya, N., de Jong, A.P.H., Goriounova, N.A., Habets, R.L.P., Takai, Y., Borst, J.G., et al. (2010). Doc2b is a high-affinity Ca2+ sensor for spontaneous neurotransmitter release. Science *327*, 1614–1618. https://doi.org/10.1126/science.1183765.
22. Xu, J., Pang, Z.P., Shin, O.-H., and Südhof, T.C. (2009). Synaptotagmin-1 functions as a Ca2+ sensor for spontaneous release. Nat. Neurosci. *12*, 759–766. https://doi.org/10.1038/nn.2320.
23. Pang, Z.P., Bacaj, T., Yang, X., Zhou, P., Xu, W., and Südhof, T.C. (2011). Doc2 supports spontaneous synaptic transmission by a Ca2+-independent mechanism. Neuron *70*, 244–251. https://doi.org/10.1016/j.neuron.2011.03.011.
24. Littleton, J.T., Stern, M., Schulze, K., Perin, M., and Bellen, H.J. (1993). Mutational analysis of Drosophila synaptotagmin demonstrates its essential role in Ca(2+)-activated neurotransmitter release. Cell *74*, 1125–1134.
25. Bergquist, F., Niazi, H.S., and Nissbrandt, H. (2002). Evidence for different exocytosis pathways in dendritic and terminal dopamine release in vivo. Brain Res. *950*, 245–253. https://doi.org/10.1016/S0006-8993(02)03047-0.
26. Rice, M.E., and Patel, J.C. (2015). Somatodendritic dopamine release: recent mechanistic insights. Philos. Trans. R. Soc. Lond. B Biol. Sci. *370*, 20140185.
27. Liu, C., Kershberg, L., Wang, J., Schneeberger, S., and Kaeser, P.S. (2018). Dopamine secretion is mediated by sparse active zone-like release sites. Cell *172*, 706–718.e15. https://doi.org/10.1016/j.cell.2018.01.008.
28. Banerjee, A., Imig, C., Balakrishnan, K., Kershberg, L., Lipstein, N., Uronen, R.-L., Wang, J., Cai, X., Benseler, F., Rhee, J.S., et al. (2022). Molecular and functional architecture of striatal dopamine release sites. Neuron *110*, 248–265.e9. https://doi.org/10.1016/j.neuron.2021.10.028.

29. Banerjee, A., Lee, J., Nemcova, P., Liu, C., and Kaeser, P.S. (2020). Synaptotagmin-1 is the Ca2+ sensor for fast striatal dopamine release. Elife *9*, e58359. https://doi.org/10.7554/eLife.58359.

30. Delignat-Lavaud, B., Ducrot, C., Kouwenhoven, W., Feller, N., and Trudeau, L.É. (2022). Implication of synaptotagmins 4 and 7 in activity-dependent somatodendritic dopamine release in the ventral midbrain. Open Biol. *12*, 210339.. https://doi.org/10.1098/rsob.210339.

31. Hikima, T., Witkovsky, P., Khatri, L., Chao, M.V., and Rice, M.E. (2022). Synaptotagmins 1 and 7 play complementary roles in somatodendritic dopamine release. J. Neurosci. *42*, 3919–3930. https://doi.org/10.1523/JNEUROSCI.2416-21.2022.

32. Mendez, J.A., Bourque, M.-J., Fasano, C., Kortleven, C., and Trudeau, L.-E. (2011). Somatodendritic dopamine release requires synaptotagmin 4 and 7 and the participation of voltage-gated calcium channels. J. Biol. Chem. *286*, 23928–23937. https://doi.org/10.1074/jbc.M111.218032.

33. Chen, B.T., Patel, J.C., Moran, K.A., and Rice, M.E. (2011). Differential calcium dependence of axonal versus somatodendritic dopamine release, with characteristics of both in the ventral tegmental area. Front. Syst. Neurosci. *5*, 39. https://doi.org/10.3389/fnsys.2011.00039.

34. Ford, C.P., Phillips, P.E.M., and Williams, J.T. (2009). The time course of dopamine transmission in the ventral tegmental area. J. Neurosci. *29*, 13344–13352. https://doi.org/10.1523/JNEUROSCI.3546-09.2009.

35. Kaeser, P.S., Deng, L., Wang, Y., Dulubova, I., Liu, X., Rizo, J., and Südhof, T.C. (2011). RIM proteins tether Ca2+ channels to presynaptic active zones via a direct PDZ-domain interaction. Cell *144*, 282–295. https://doi.org/10.1016/j.cell.2010.12.029.

36. Deng, L., Kaeser, P.S., Xu, W., and Südhof, T.C. (2011). RIM proteins activate vesicle priming by reversing autoinhibitory homodimerization of Munc13. Neuron *69*, 317–331. https://doi.org/10.1016/j.neuron.2011.01.005.

37. Müller, M., Liu, K.S.Y., Sigrist, S.J., and Davis, G.W. (2012). RIM controls homeostatic plasticity through modulation of the readily-releasable vesicle pool. J. Neurosci. *32*, 16574–16585. https://doi.org/10.1523/JNEUROSCI.0981-12.2012.

38. Han, Y., Babai, N., Kaeser, P., Südhof, T.C., and Schneggenburger, R. (2015). RIM1 and RIM2 redundantly determine Ca 2+ channel density and readily releasable pool size at a large hindbrain synapse. J. Neurophysiol. *113*, 255–263. https://doi.org/10.1152/jn.00488.2014.

39. Gracheva, E.O., Hadwiger, G., Nonet, M.L., and Richmond, J.E. (2008). Direct interactions between C. elegans RAB-3 and Rim provide a mechanism to target vesicles to the presynaptic density. Neurosci. Lett. *444*, 137–142. https://doi.org/10.1016/j.neulet.2008.08.026.

40. Han, Y., Kaeser, P.S., Südhof, T.C., and Schneggenburger, R. (2011). RIM determines Ca^2+ channel density and vesicle docking at the presynaptic active zone. Neuron *69*, 304–316. https://doi.org/10.1016/j.neuron.2010.12.014.

41. Kaeser, P.S., Deng, L., Fan, M., and Südhof, T.C. (2012). RIM genes differentially contribute to organizing presynaptic release sites. Proc. Natl. Acad. Sci. USA *109*, 11830–11835. https://doi.org/10.1073/pnas.1209318109.

42. Robinson, B.G., Cai, X., Wang, J., Bunzow, J.R., Williams, J.T., and Kaeser, P.S. (2019). RIM is essential for stimulated but not spontaneous somatodendritic dopamine release in the midbrain. Elife *8*, e47972. https://doi.org/10.7554/eLife.47972.

43. Saunders, A., Macosko, E.Z., Wysoker, A., Goldman, M., Krienen, F.M., de Rivera, H., Bien, E., Baum, M., Bortolin, L., Wang, S., et al. (2018). Molecular diversity and specializations among the cells of the adult mouse brain. Cell *174*, 1015–1030.e16. https://doi.org/10.1016/j.cell.2018.07.028.

44. Lein, E.S., Hawrylycz, M.J., Ao, N., Ayres, M., Bensinger, A., Bernard, A., Boe, A.F., Boguski, M.S., Brockway, K.S., Byrnes, E.J., et al. (2007). Genome-wide atlas of gene expression in the adult mouse brain. Nature *445*, 168–176. https://doi.org/10.1038/nature05453.

45. Zhou, Q., Lai, Y., Bacaj, T., Zhao, M., Lyubimov, A.Y., Uervirojnangkoorn, M., Zeldin, O.B., Brewster, A.S., Sauter, N.K., Cohen, A.E., et al. (2015). Architecture of the synaptotagmin–SNARE machinery for neuronal exocytosis. Nature *525*, 62–67. https://doi.org/10.1038/nature14975.

46. Bäckman, C.M., Malik, N., Zhang, Y., Shan, L., Grinberg, A., Hoffer, B.J., Westphal, H., and Tomac, A.C. (2006). Characterization of a mouse strain expressing Cre recombinase from the 3' untranslated region of the dopamine transporter locus. Genesis *44*, 383–390. https://doi.org/10.1002/dvg.20228.

47. Kershberg L., Banerjee A., Kaeser P.S. Protein composition of axonal dopamine release sites in the striatum. 2022. ELife. https://doi.org/10.1101/2022.08.31.505994.

48. Wassef, M., Berod, A., and Sotelo, C. (1981). Dopaminergic dendrites in the pars reticulata of the rat substantia nigra and their striatal input. Combined immunocytochemical localization of tyrosine hydroxylase and anterograde degeneration. Neuroscience *6*, 2125–2139. https://doi.org/10.1016/0306-4522(81)90003-8.

49. Bayer, V.E., and Pickel, V.M. (1990). Ultrastructural localization of tyrosine hydroxylase in the rat ventral tegmental area: relationship between immunolabeling density and neuronal associations. J. Neurosci. *10*, 2996–3013.

50. Deutch, A.Y., Goldstein, M., Baldino, F., and Roth, R.H. (1988). Telencephalic projections of the A8 dopamine cell group. Ann. N. Y. Acad. Sci. *537*, 27–50. https://doi.org/10.1111/j.1749-6632.1988.tb42095.x.

51. Beckstead, M.J., Ford, C.P., Phillips, P.E.M., and Williams, J.T. (2007). Presynaptic regulation of dendrodendritic dopamine transmission. Eur. J. Neurosci. *26*, 1479–1488. https://doi.org/10.1111/j.1460-9568.2007.05775.x.

52. Patriarchi, T., Cho, J.R., Merten, K., Howe, M.W., Marley, A., Xiong, W.-H., Folk, R.W., Broussard, G.J., Liang, R., Jang, M.J., et al. (2018). Ultrafast neuronal imaging of dopamine dynamics with designed genetically encoded sensors. Science *360*, eaat4422. https://doi.org/10.1126/science.aat4422.

53. Zucker, R.S., and Regehr, W.G. (2002). Short-term synaptic plasticity. Annu. Rev. Physiol. *64*, 355–405. https://doi.org/10.1146/annurev.physiol.64.092501.11454764/1/355.

54. Lin, J.Y., Lin, M.Z., Steinbach, P., and Tsien, R.Y. (2009). Characterization of engineered channelrhodopsin variants with improved properties and kinetics. Biophys. J. *96*, 1803–1814. https://doi.org/10.1016/j.bpj.2008.11.034.

55. Maximov, A., and Südhof, T.C. (2005). Autonomous function of synaptotagmin 1 in triggering synchronous release independent of asynchronous release. Neuron *48*, 547–554. https://doi.org/10.1016/j.neuron.2005.09.006.

56. Xu, W., Morishita, W., Buckmaster, P.S., Pang, Z.P., Malenka, R.C., and Südhof, T.C. (2012). Distinct neuronal coding schemes in memory revealed by selective erasure of fast synchronous synaptic transmission. Neuron *73*, 990–1001. https://doi.org/10.1016/j.neuron.2011.12.036.

57. Gantz, S.C., Bunzow, J.R., and Williams, J.T. (2013). Spontaneous inhibitory synaptic currents mediated by a G protein-coupled receptor. Neuron *78*, 807–812. https://doi.org/10.1016/j.neuron.2013.04.013.

58. Bouazza-Arostegui, B., Camacho, M., Brockmann, M.M., Zobel, S., and Rosenmund, C. (2022). Deconstructing synaptotagmin-1's distinct roles in synaptic vesicle priming and neurotransmitter release. J. Neurosci. *42*, 2856–2871. https://doi.org/10.1523/JNEUROSCI.1945-21.2022.

59. Chen, B.T., and Rice, M.E. (2001). Novel Ca2+ dependence and time course of somatodendritic dopamine release: substantia nigra versus striatum. J. Neurosci. *21*, 7841–7847.

60. Dai, H., Shin, O.-H., Machius, M., Tomchick, D.R., Südhof, T.C., and Rizo, J. (2004). Structural basis for the evolutionary inactivation of Ca2+ binding to synaptotagmin 4. Nat. Struct. Mol. Biol. *11*, 844–849. https://doi.org/10.1038/nsmb817.

61. Wang, Z., and Chapman, E.R. (2010). Rat and Drosophila synaptotagmin 4 have opposite effects during SNARE-catalyzed membrane fusion. J. Biol. Chem. *285*, 30759–30766. https://doi.org/10.1074/jbc.M110.137745.

62. Kissiwaa, S.A., Lebowitz, J.J., Engeln, K.A., Bowman, A.M., Williams, J.T., and Jackman, S.L. (2021). Synaptotagmin-7 enhances phasic dopamine release. Preprint at bioRxiv. https://doi.org/10.1101/2021.10.17.464710.

63. Hikima, T., Lee, C.R., Witkovsky, P., Chesler, J., Ichtchenko, K., and Rice, M.E. (2021). Activity-dependent somatodendritic dopamine release in the substantia nigra autoinhibits the releasing neuron. Cell Rep. *35*, 108951. https://doi.org/10.1016/j.celrep.2021.108951.

64. Delignat-Lavaud, B., Kano, J., Ducrot, C., Massé, I., Mukherjee, S., Giguère, N., Moquin, L., Lévesque, C., Nanni, S.B., Bourque, M.-J., et al. (2021). The calcium sensor synaptotagmin-1 is critical for phasic axonal dopamine release in the striatum and mesencephalon, but is dispensable for basic motor behaviors in mice. Preprint at bioRxiv. https://doi.org/10.1101/2021.09.15.460511.

65. Liu, C., Goel, P., and Kaeser, P.S. (2021). Spatial and temporal scales of dopamine transmission. Nat. Rev. Neurosci. *22*, 345–358. https://doi.org/10.1038/s41583-021-00455-7.

66. Biederer, T., Kaeser, P.S., and Blanpied, T.A. (2017). Transcellular nanoalignment of synaptic function. Neuron *96*, 680–696. https://doi.org/10.1016/j.neuron.2017.10.006.

67. Condon, A.F., Robinson, B.G., Asad, N., Dore, T.M., Tian, L., and Williams, J.T. (2021). The residence of synaptically released dopamine on D2 autoreceptors. Cell Rep. *36*, 109465. https://doi.org/10.1016/j.celrep.2021.109465.

68. Bixby, J.L., and Reichardt, L.F. (1985). The expression and localization of synaptic vesicle antigens at neuromuscular junctions in vitro. J. Neurosci. *5*, 3070–3080.

69. Takamori, S., Holt, M., Stenius, K., Lemke, E.A., Grønborg, M., Riedel, D., Urlaub, H., Schenck, S., Brügger, B., Ringler, P., et al. (2006). Molecular anatomy of a trafficking organelle. Cell *127*, 831–846. https://doi.org/10.1016/j.cell.2006.10.030.

70. Sugita, S., Han, W., Butz, S., Liu, X., Fernández-Chacón, R., Lao, Y., and Südhof, T.C. (2001). Synaptotagmin VII as a plasma membrane Ca(2+) sensor in exocytosis. Neuron *30*, 459–473. https://doi.org/10.1016/s0896-6273(01)00290-2.

71. Chakrabarti, S., Kobayashi, K.S., Flavell, R.a., Marks, C.B., Miyake, K., Liston, D.R., Fowler, K.T., Gorelick, F.S., and Andrews, N.W. (2003). Impaired membrane resealing and autoimmune myositis in synaptotagmin VII-deficient mice. J. Cell Biol. *162*, 543–549. https://doi.org/10.1083/jcb.200305131.

72. Fortin, G.D., Desrosiers, C.C., Yamaguchi, N., and Trudeau, L.E. (2006). Basal somatodendritic dopamine release requires snare proteins. J. Neurochem. *96*, 1740–1749. https://doi.org/10.1111/j.1471-4159.2006.03699.x.

73. Chen, B.T., Moran, K.A., Avshalumov, M.V., and Rice, M.E. (2006). Limited regulation of somatodendritic dopamine release by voltage-sensitive Ca channels contrasted with strong regulation of axonal dopamine release. J. Neurochem. *96*, 645–655. https://doi.org/10.1111/j.1471-4159.2005.03519.x.

74. Ford, C.P., Gantz, S.C., Phillips, P.E.M., and Williams, J.T. (2010). Control of extracellular dopamine at dendrite and axon terminals. J. Neurosci. *30*, 6975–6983. https://doi.org/10.1523/JNEUROSCI.1020-10.2010.

75. Nirenberg, M.J., Chan, J., Liu, Y., Edwards, R.H., and Pickel, V.M. (1996). Ultrastructural localization of the vesicular monoamine transporter-2 in midbrain dopaminergic neurons: potential sites for somatodendritic storage and release of dopamine. J. Neurosci. *16*, 4135–4145.

76. Pickel, V.M., Chan, J., and Nirenberg, M.J. (2002). Region-specific targeting of dopamine D2-receptors and somatodendritic vesicular monoamine transporter 2 (VMAT2) within ventral tegmental area subdivisions. Synapse *45*, 113–124. https://doi.org/10.1002/syn.10092.

77. Mercer, L., del Fiacco, M., and Cuello, A.C. (1979). The smooth endoplasmic reticulum as a possible storage site for dendritic dopamine in substantia nigra neurones. Experientia *35*, 101–103. https://doi.org/10.1007/BF01917903.

78. Liu, C., and Kaeser, P.S. (2019). Mechanisms and regulation of dopamine release. Curr. Opin. Neurobiol. *57*, 46–53. https://doi.org/10.1016/j.conb.2019.01.001.

79. Uchigashima, M., Ohtsuka, T., Kobayashi, K., and Watanabe, M. (2016). Dopamine synapse is a neuroligin-2-mediated contact between dopaminergic presynaptic and GABAergic postsynaptic structures. Proc. Natl. Acad. Sci. USA *113*, 4206–4211. https://doi.org/10.1073/pnas.1514074113.

80. Wildenberg, G., Sorokina, A., Koranda, J., Monical, A., Heer, C., Sheffield, M., Zhuang, X., McGehee, D., and Kasthuri, B. (2021). Partial connectomes of labeled dopaminergic circuits reveal non-synaptic communication and axonal remodeling after exposure to cocaine. Elife *10*, e71981. https://doi.org/10.7554/eLife.71981.

81. Skarnes, W.C., Rosen, B., West, A.P., Koutsourakis, M., Bushell, W., Iyer, V., Mujica, A.O., Thomas, M., Harrow, J., Cox, T., et al. (2011). A conditional knockout resource for the genome-wide study of mouse gene function. Nature *474*, 337–342. https://doi.org/10.1038/nature10163.

82. Zhou, Q., Zhou, P., Wang, A.L., Wu, D., Zhao, M., Südhof, T.C., and Brunger, A.T. (2017). The primed SNARE-complexin-synaptotagmin complex for neuronal exocytosis. Nature *548*, 420–425. https://doi.org/10.1038/nature23484.

83. Kochubey, O., Babai, N., and Schneggenburger, R. (2016). A synaptotagmin isoform switch during the development of an identified CNS synapse. Neuron *90*, 984–999. https://doi.org/10.1016/j.neuron.2016.04.038.

84. Bouhours, B., Gjoni, E., Kochubey, O., and Schneggenburger, R. (2017). Synaptotagmin2 (Syt2) drives fast release redundantly with Syt1 at the output synapses of parvalbumin-expressing inhibitory neurons. J. Neurosci. *37*, 4604–4617. https://doi.org/10.1523/JNEUROSCI.3736-16.2017.

STAR★METHODS

KEY RESOURCES TABLE

REAGENT or RESOURCE	SOURCE	IDENTIFIER
Chemicals, peptides, and recombinant proteins		
(+)-MK 801 maleate	Hello Bio	Cat# HB0004
NBQX	Hello Bio	Cat# HB0442
CGP55845 hydrochloride	Hello Bio	Cat# HB0960
Picrotoxin	Hello Bio	Cat# HB0506
Tetrodotoxin citrate	Tocris	Ca# 1069
Experimental models: Cell lines		
HEK293T cells	ATCC	Cat#: CRL-3216 RRID: CVCL_0063
Experimental models: Organisms/strains		
Mouse: Syt-1 floxed; generated from C57BL/6Ntac-$^{Syt1tm1a(EUCOMM)Wtsi}$/WtsiCnrm	Zhou et al.[45]	EMMA ID EM:06829, RRID:IMSR_EM:06829; the identifier refers to the line before flp recombination
Mouse: B6.SJL-Slc6a3$^{tm1.1(cre)Bkmm}$/J; DAT$^{IRES-Cre}$	Backman et al.[46]	JAX 006660, RRID: IMSR_JAX:006660
Recombinant DNA		
pAAV-hSyn-FLEX-oChIEF-citrine-P2A-Syt-1	This paper; Kaeser lab, plasmid was used to generate AAVs.	lab plasmid code (LPC): p869
pAAV-hSyn-FLEX-oChIEF-citrine	Addgene, Lin et al.,[54] plasmid was used to generate AAVs.	Plasmid# 50973, RRID:Addgene 50973; LPC: p901
pFB-CAG-SNAP-hD2Rshort-P2A-GFP	This paper; ViroVek, plasmid was used to generate AAVs.	LPC: p1038
Software and algorithms		
AxoGraph	AxoGraph	RRID:SCR_014284; https://www.axograph.com
LabChart	AD Instruments	https://www.adinstruments.com/products/labchart
Prism 9	GraphPad	RRID: SCR_002798; https://www.graphpad.com

RESOURCE AVAILABILITY

Lead contact

Further information and requests for resources and reagents should be directed to and will be fulfilled by the Lead contact, Pascal S. Kaeser (kaeser@hms.harvard.edu).

Materials availability

Plasmids generated for this study will be shared within limits of respective material transfer agreements. AAVs are exhaustible and will be shared as long as they are available and within limits of respective material transfer agreements. Mouse mutant alleles are publicly available as outlined in the key resources table.

Data and code availability

- Data reported in this paper will be shared by the lead contact upon request.
- This paper does not report original code.
- Any additional information required to reanalyze the data reported in this paper is available from the lead contact upon request.

EXPERIMENTAL MODEL AND SUBJECT DETAILS

Animals

Conditional knockout mice for Syt-1 in dopamine neurons were generated through mouse breeding as described before,[29] crossing Syt-1^{floxed} mice[45] with DAT$^{IRES-Cre}$ mice,[46] and striatal phenotypes were described.[29,47] Syt-1^{floxed} mice were generated from a gene

targeting experiment (C57BL/6Ntac-$^{Syt1tm1a(EUCOMM)Wtsi}$/WtsiCnrm) for coding exon 2 (if non-coding exons are included in the numbering, the corresponding exon number is exon 6),[45,81] and further characterized in.[82–84] In all experiments, Syt-1 cKO^{DA} mice are mice homozygote for Syt-1 floxed (Syt-1$^{f/f}$) alleles and with a heterozygote allele for DAT$^{IRES-Cre}$; Syt-1 control mice are littermate mice or age-matched mice from the same breedings with homozygote Syt-1 wild type alleles (Syt-1$^{+/+}$) and a heterozygote allele for DAT$^{IRES-Cre}$. Male and female adult mice (25–45 weeks old) were used for all experiments. Genotype comparisons were performed by an experimentalist blind to genotype, and unblinding of genotypes was done after experiments and analyses were completed. All animal experiments were performed according to protocols approved by the respective Animal Care and Use Committee at Harvard University and at Oregon Health and Science University.

Cell lines

HEK293T cells were purchased from ATCC (CRL-3216, RRID: CVCL_0063, an immortalized, authenticated cell line of female origin). The cells were expanded and stored as stock vials in liquid nitrogen. They were thawed for use and were grown in Dulbecco's Modified Eagle Medium (DMEM) with 10% fetal bovine serum (Atlas Biologicals F-0500-D) and 1% Penicillin-Streptomycin. The cells were grown in a tissue culture incubator set to 37°C and 5% CO_2, and they were passaged every 2 to 3 days at a ratio of 1:5 to 1:7. Each batch of cells was replaced after ~20 passages with cells thawed from a fresh stock vial.

METHOD DETAILS

Molecular biology and production of AAV viruses

Adeno-associated viruses (AAVs) were either generated in the lab or by ViroVek (Hayward, CA). All AAVs were of the AAV9 serotype and genomic titers ranged from 1.43×10^{12} to 2.15×10^{13} viral genome copies/mL. Cre-dependent AAVs were injected in the substantia nigra for expression of oChIEF-citrine with or without Syt-1. For expression oChIEF-citrine alone, pAAV-hSyn-FLEX-oChIEF-citrine[54] (RRID:Addgene_50973, LPC: p901) was used; the following protein is encoded (numbered in subscript according to amino acid sequences of GenBank KF437396.1 for oChIEF and GenBank MK301208.1 for citrine): $_{oChIEF,1}$MVSR … YESS$_{359}$-LE-$_{citrine,1}$MVSKG … ELYK$_{239}$. For co-expression of oChIEF and synaptotagmin-1, we constructed an AAV vector, pAAV-hSyn-FLEX-oChIEF-citrine-P2A-Syt-1 (LPC: p869) producing citrine-tagged oChIEF and rat synaptotagmin-1. The following two proteins are encoded (numbered in subscript according to amino acid sequences of GenBank KF437396.1 for oChIEF, GenBank MK301208.1 for citrine, and NCBI Ref Seq NM_001033680.2 for Syt-1): $_{oChIEF,1}$MVSR … YESS$_{359}$-LEG-$_{citrine,2}$VSKG … ELYK$_{239}$-GAPGSGATNFSLLKQAGDVEENPG and PAPL-$_{Syt\text{-}1,2}$VSAS … AVKK$_{421}$. AAVs were generated in HEK293T cells in the lab using calcium phosphate transfection. Cells were collected and lysed 72 h after transfection. AAV viral particles were extracted and purified from the 40% layer after iodixanol gradient ultracentrifugation. An AAV encoding the short version of the human D2 receptor (hD2R$_S$) was generated by ViroVek (Hayward, CA). A plasmid encoding an SNAP-tagged (at the N-terminus) hD2R$_S$ and a cytosolic GFP (via a P2A sequence) was generated and provided to ViroVek. This plasmid was subcloned to generate pFB-CAG-SNAP-hD2Rshort-P2A-GFP (LPC: p1038). The following two proteins are encoded (numbered in subscript according to amino acid sequences of GenBank KM043782.1 for the SNAPtag, NCBI Ref Seq NM_016574.4 for hD2Rshort, and GenBank MF405194.1 for GFP): MKTIIALSYIFCLVFADYKDDDDA-$_{SNAPtag,172}$MDKD … PGLG$_{353}$-$_{hD2Rshort,1}$MDPL … ILHC$_{414}$-SGSGATNFSLLKQAGDVEENPG and P-$_{GFP,1}$MVSK … ELYK$_{239}$. After verification, the plasmid was used by ViroVek for AAV production.

Stereotaxic viral delivery

Mice (postnatal days 56–115) were anesthetized and placed in a stereotaxic frame for midbrain injections of AAV viruses. Anesthesia was maintained throughout surgery with isoflurane. 120 nL of AAV was injected bilaterally into the ventral midbrain at a rate of 0.1 μL/min using an UltraMicroPump3 microinjection syringe pump (World Precision Instruments, Sarasota FL) controlled by a Wizard 211 digital readout system (ANILAM Inc., Jamestown NY). Injection coordinates were (in mm): 2.3 posterior from bregma; ± 1.3 lateral from midline; 4.5 below pia. Post-operative analgesia was provided following approved protocols. Experiments with AAV-mediated D2 receptor expression were performed 10 to 20 days after surgery. Experiments with oChIEF-citrine expression (and for the rescue condition Syt-1 co-expression) were performed 20 to 30 days after surgery.

Brain slice preparation

Mice (25–45 weeks old) were anesthetized with isoflurane and decapitated, and the brain was collected in 32–35°C warm Krebs buffer containing (in mM): 126 NaCl, 2.5 KCl, 1.2 $MgCl_2$, 2.4 $CaCl_2$, 1.4 NaH_2PO_4, 25 $NaHCO_3$, and 11 Dextrose. The Krebs buffer used for extraction, cutting, and recovery contained 10 μM MK-801 to prevent NMDA-mediated excitotoxic damage. 222 μm thick horizontal slices containing the midbrain were cut using a vibrating microtome in warm Krebs buffer bubbled with 95% O_2/5% CO_2 and slices were allowed to recover in the same buffer at 30°C for ≥30 min before recordings. Prior to recordings, slices were hemisected along the midline to record from each side separately. For recording, the hemisected slice was transferred to the recording chamber, which was continuously perfused at 2 to 3 mL/min with bubbled Krebs buffer at 34°C. All experiments were completed within 7 h of slicing.

Electrophysiological recordings in brain slices

SNc dopamine neurons were identified by their morphology and by their localization lateral to the medial terminal nucleus of the accessory optic system. D2-IPSCs were recorded following previously established protocols.[10,42,57] Specifically, experiments were conducted in Krebs buffer with the addition of NBQX (600 nM), CGP55845 (300 nM), and picrotoxin (100 μM). Recordings were made using glass pipettes (1.0–2.5 MΩ) filled with an internal solution containing (in mM): 100 K-methanesulphonate, 20 NaCl, 1.5 $MgCl_2$, 10 HEPES (K), 2 ATP, 0.2 GTP, 10 phosphocreatine, and 10 BAPTA (4K). The recorded cells exhibited ~1–5 Hz spontaneous firing as assessed in cell-attached configuration, and firing rates were recorded and analyzed in a subset of experiments in cell attached mode with an amplitude threshold. After break-in, cells were voltage-clamped at −55 mV and resistance and capacitance were monitored; cells with a series resistance ≥12 MΩ were discarded. A focal monopolar or bipolar stimulation electrode was used to stimulate the cells with a current of ~50–250 μA once per min. The typical distance of the stimulation electrode to the recorded cell was 50–100 μm. For assessment of evoked release, the stimulation intensity was set such that a D2-IPSC was detected in response to five stimuli at 40 Hz, and only cells with a detectable 5-stimulus D2-IPSC were included. The number and frequency of electrical stimuli varied, and the stimulation protocol is described in each figure; if multiple stimulus protocols were used for a given cell, the order was randomized but stimulation intensity was kept identical across protocols. For optogenetic stimulation, a 470 nm LED (Thorlabs) was used to deliver paired flashes of blue light (2 mW, 25 ms, 0.4 Hz) through a 40× water-immersion objective directly over the recorded cell. As with electrical stimulation, paired light flashes were delivered once per minute. All data reported for stimulated D2-IPSCs reflect the average of three consecutive sweeps. Analyses of spontaneous D2-IPSCs were constrained to the intervals between stimuli or after stimulus protocols were completed. These recordings were performed in the same solutions as described above for most cells; for a subset of cells, 1 μM TTX was added or the extracellular solution contained 0.5 mM $CaCl_2$ and 5 mM $MgCl_2$ instead of 2.4 $CaCl_2$ and 1.2 $MgCl_2$. Data acquisition was performed with AxoGraph (Berkley, CA) and recordings were monitored with LabChart (AD instruments, Colorado Springs, CO). D2-IPSC amplitudes were measured as the average of a 20 ms window centered around the peak outward current determined in AxoGraph. The charge transfer was quantified as the area under the curve starting at stimulation for 1.5 s, at which time the D2-IPSC returned to baseline. Paired pulse ratios were calculated as the ratio of the second D2-IPSC peak to the first. In rescue experiments, we used optogenetic activation to assess the D2-oIPSC for each recorded cell. We then used electrical stimulation to assess rescue and only included cells for which the D2-oIPSC amplitude was equal to or greater than that of the D2-IPSC generated by a single electrical stimulus to select for cells with robust viral expression in the inputs. Spontaneous D2-IPSCs were identified using a sliding template in AxoGraph as described previously.[42,57] The template was based on the shape of the D2-IPSC and used the following parameters: a 50 ms baseline, a rise time (10–90%) of 50 ms, and a decay τ of 200 ms. The threshold for event detection was 3.7 times the standard deviation of baseline noise for events that fit the waveform of the sliding template, and events had to be separated by a minimum of 300 ms. For all experiments examining spontaneous D2-IPSCs and several experiments examining evoked D2-IPSCs, sulpiride was added at the end of the recording period to inhibit D2 receptors, which led to a block of spontaneous and evoked D2-IPSCs, respectively, as established before.[10,57] Data acquisition and analyses were conducted by experimenters blind to genotype.

QUANTIFICATION AND STATISTICAL ANALYSIS

Data are displayed as mean ± SEM with individual values as circles, and statistical significance is denoted as $^*p < 0.05$, $^{**}p < 0.01$, and $^{***}p < 0.005$ in the figures. Representative traces except for those of spontaneous D2-IPSCs are the average of three consecutive sweeps. Statistical testing was performed in GraphPad Prism 9 (GraphPad, San Diego, CA). For statistical analyses, each cell was considered an observation because the technical nature of these recordings precluded getting sufficient numbers of cells per mouse for averaging per mouse. Datasets were tested for normality with a Shapiro-Wilk test. For comparison of two groups with a single variable, normally distributed data were assessed with unpaired Student's t-tests, and non-normally distributed data with Mann-Whitney rank sum tests. For spontaneous D2-IPSC analyses, a two-way ANOVA was used. Sample sizes, statistical tests used, and significance are reported for all data in the corresponding figures and figure legends.

Cell Reports, Volume *42*

Supplemental information

Synaptotagmin-1 is a Ca^{2+} sensor for somatodendritic dopamine release

Joseph J. Lebowitz, Aditi Banerjee, Claire Qiao, James R. Bunzow, John T. Williams, and Pascal S. Kaeser

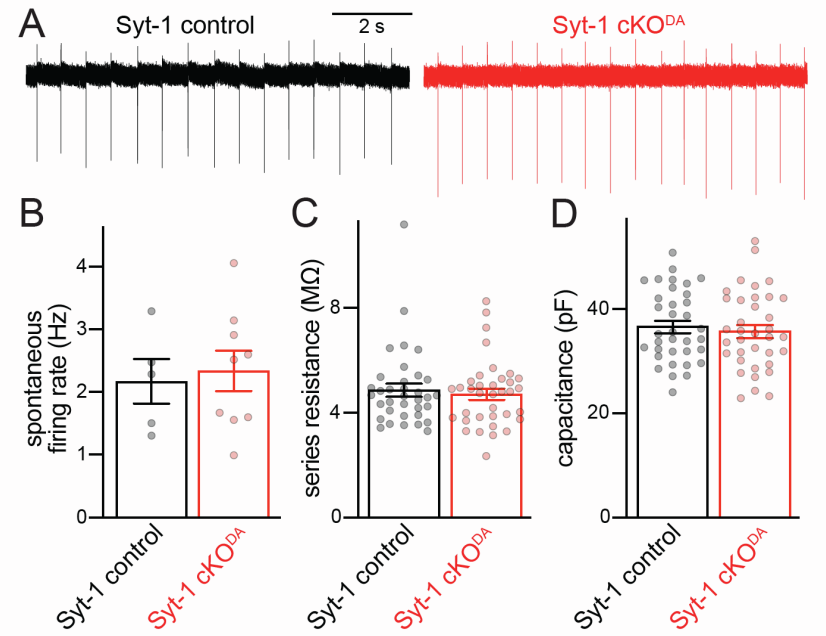

Figure S1. Basal electrical properties are unchanged in Syt-1 cKO^{DA} mice, related to Fig. 1.

A, B. Example traces (A) and quantification of spontaneous firing rate (B) recorded in cell-attached mode prior to break-in, measured over a one-minute period, Syt-1 control 5 cells/3 mice, Syt-1 cKO^{DA} 9 cells/3 mice.

C, D. Quantification of series resistance (C) and capacitance (D) measured following break-in, Syt-1 control 35 cells/8 mice, Syt-1 cKO^{DA} 36 cells/8 mice.

Data are mean ± SEM; no significant differences were observed as determined by unpaired Student's t-tests (B, D) or a Mann Whitney rank sum test (C).

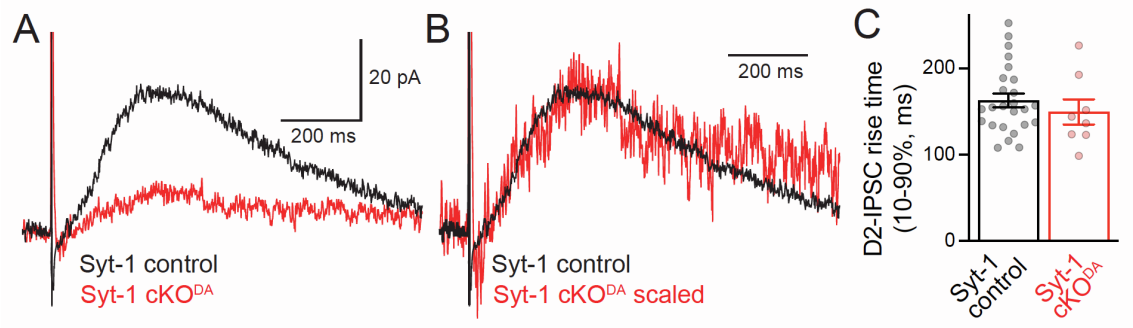

Figure S2. Assessment of D2-IPSC rise times in Syt-1 cKO^{DA} mice, related to Fig. 1.

A-C. Absolute (A) and scaled (B) example traces and quantification of 10-90% rise time of single-stimulus D2-IPSCs of the recordings shown in Figs. 1D and 1G, Syt-1 control 25 cells/7 mice, Syt-1 cKO^{DA} 8 cells/5 mice. Only D2-IPSCs larger than 10 pA were included. Because of the strong reduction in the D2-IPSC amplitude after Syt-1 ablation, there are fewer observations for Syt-1 cKO^{DA}. The kinetics of the D2-IPSC are dominated by the time course of GPCR signaling and are unlikely to reflect release kinetics.

Data are mean ± SEM; no significant differences were observed as determined by unpaired Student's t-test (C).

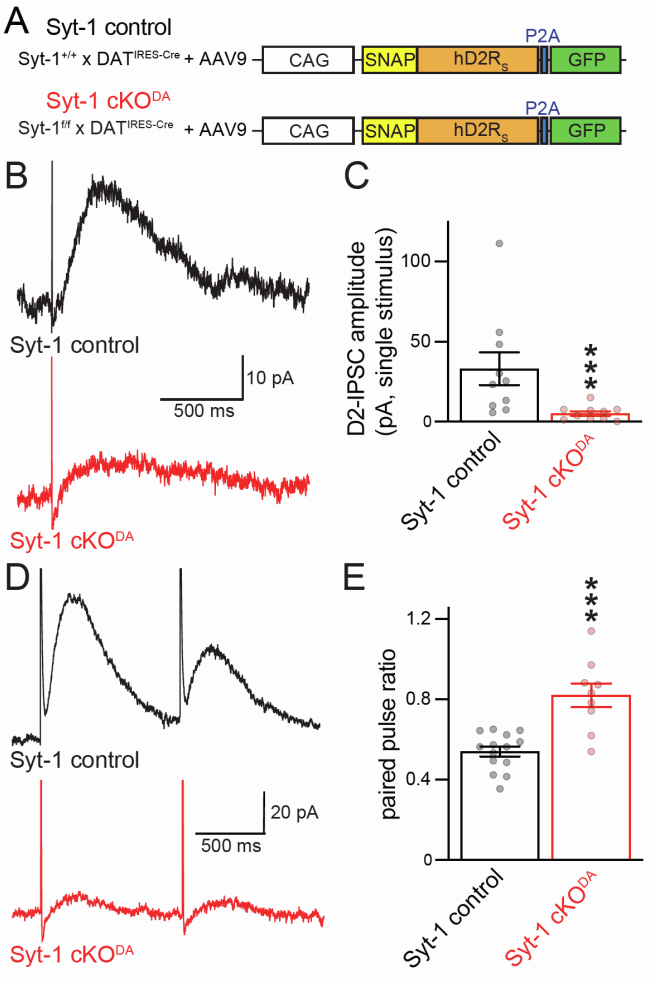

Figure S3. D2 receptor overexpression does not alter evoked D2-IPSCs, related to Fig. 4.

A. Strategy for AAV-mediated overexpression of D2 receptors (human, short version, $hD2R_S$) in the midbrain.

B, C. Example traces (B) and quantification (C) of D2-IPSCs evoked by single stimuli after overexpression of D2 receptors, Syt-1 control 10 cells/3 mice, Syt-1 cKO^{DA} 10 cells/4 mice.

D, E. Example traces (D) and quantification of paired pulse ratios (E) of D2-IPSCs evoked by two stimuli (1-s interval) after D2 receptor overexpression**,** Syt-1 control 14 cells/7 mice, Syt-1 cKO^{DA} 9 cells/5 mice.

Data are mean ± SEM; ***$p < 0.005$, statistical significance determined by a Mann Whitney rank sum test (C) or an unpaired Student's t-test (E). Overall, D2-IPSCs are similar compared to experiments without D2 receptor overexpression (Fig. 1) in both genotypes.